Mechanistic and Structural Contributions of Critical Surface and Internal Residues to Cytochrome *c* Electron Transfer Reactivity†

Steven P. Rafferty,‡,§ J. Guy Guillemette,‡,||,⊥ Albert M. Berghuis,‡,# Michael Smith,‡,|| Gary D. Brayer,*,‡ and A. Grant Mauk*,‡

Department of Biochemistry and Molecular Biology and the Biotechnology Laboratory, University of British Columbia, Vancouver, British Columbia, Canada V6T 1Z3

Received February 22, 1996; Revised Manuscript Received June 17, 1996⊗

ABSTRACT: The influence of mutations in two conserved regions of yeast iso-1-cytochrome *c* believed to be critical to the mechanism of cytochrome *c* electron transfer reactions has been investigated. The variants Asn52Ala, Tyr67Phe, Ile75Met, and Thr78Gly involve perturbation of critical hydrogen-bonding interactions with an internal water molecule (Wat166) and have been studied in terms of their electrochemical properties and the kinetics with which they are reduced by $Fe(EDTA)^{2-}$ and oxidized by $Co(phen)_3^{3+}$. In parallel studies, the $Co(phen)_3^{3+}$ oxidation kinetics of Tyr, Leu, Ile, Ala, Ser, and Gly variants of the phylogenetically conserved residue Phe82 have been studied and correlated with previous electrochemical and kinetic results. To assist mechanistic interpretation of these results, the three-dimensional structures of the Asn52Ala and Ile75Met ferrocytochrome *c* variants have been determined. The reduction potentials of the variants modified in the region of Wat166 were at least 33 mV (pH 6, 25 °C, and $\mu = 0.1$ M) lower than that of the wild-type protein. Electron transfer reactivity of this family of variants in both the oxidation and reduction reactions was increased as much as 10-fold over that of the wild-type cytochrome. On the other hand, the reactivity of the position-82 variants in both oxidation and reduction depended on the structural characteristics of the oxidation−reduction reagent with which they reacted, and this reactivity was related to the nature of the residue at this position. These findings have been interpreted as demonstrating that the principal influence of modification at position-82 arises from changes in the nature of reactant−protein interaction at the surface of the protein and in maintaining the high reduction potential of the cytochrome while the principal influence of internal modifications near Wat166 results from alteration of the reorganization energy for the oxidation state-linked conformational change defined by crystallographic analysis of the wild-type protein.

Small, well-characterized electron transfer proteins are useful models for investigation of electron transfer reactions involved in photosynthesis, respiration, and the catalytic cycles of many enzymes. In particular, mitochondrial cytochrome *c* has been studied extensively in such work (Scott & Mauk, 1996). The use of oligonucleotide-directed site specific mutation (Zoller & Smith, 1983) in the study of cytochrome *c* has been permitted by the availability of a cloned and sequenced gene encoding the yeast cytochrome (Smith et al., 1979). As a result, selectively modified variants of cytochrome *c* were first used to understand metalloprotein electron transfer reactions several years ago (Pielak et al., 1985). Since this initial work, many variant cytochromes have been constructed and characterized in functional and structural studies designed to probe the mechanism by which this protein functions (Mauk, 1990).

Conserved residues in the heme environment of cytochrome *c* are critical targets of such studies. In the present work, we have assessed the effects of replacement of two types of such residues on the oxidation−reduction equilibrium of cytochrome *c* and have used this information to interpret the kinetics of oxidation and reduction of this protein by substitutionally inert metal complexes. The first group of variants involves replacement of the invariant residue Phe82, the phenyl group of which is parallel to and ∼3.5 Å from the heme near its solvent accessible edge (Figure 1A). The structural (Louie & Brayer, 1988, 1989; Louie et al., 1988) and functional (Michel et al., 1989; Pearce et al., 1989; Rafferty et al., 1990) roles of this residue have been characterized in several previous studies. On the basis of this work, Phe82 is believed to function in maintaining the high reduction potential of the protein by contributing to or controlling the dielectric environment of the heme (Kassner, 1972, 1973; Louie & Brayer, 1989; Louie et al., 1988; Rafferty et al., 1990), in influencing electron transfer kinetics (Rafferty et al., 1990; Nocek et al., 1991), and in stabilizing the native structure of the active site (Pearce et al., 1989). In previous studies evaluating the kinetics of reduction of these variants by $Fe(EDTA)^{2-}$, the effects of perturbing the local heme environment through replacement of Phe82 were shown to result from alteration of the protein surface near

† This work was supported by NIH Grant GM33804 (to A.G.M.) and Medical Research Council of Canada Grants MT-1706 (to M.S.) and MT-7975 (to G.D.B.). S.P.R. was a recipient of an MRC of Canada Studentship. M.S. is a Medical Research Council of Canada Career Scientist.

‡ Department of Biochemistry and Molecular Biology, University of British Columbia.

§ Present address: Laboratory of Host Defenses, NIAID, National Institutes of Health, Bethesda, MD 20892.

|| Biotechnology Laboratory, University of British Columbia.

⊥ Present address: Department of Chemistry, University of Waterloo, Waterloo, Ontario, Canada N2L 3G1.

Present address: Department of Biochemistry, McMaster University, Hamilton, Ontario, Canada L8N 3Z5.

⊗ Abstract published in *Advance ACS Abstracts,* August 1, 1996.

S0006-2960(96)00430-8 CCC: $12.00

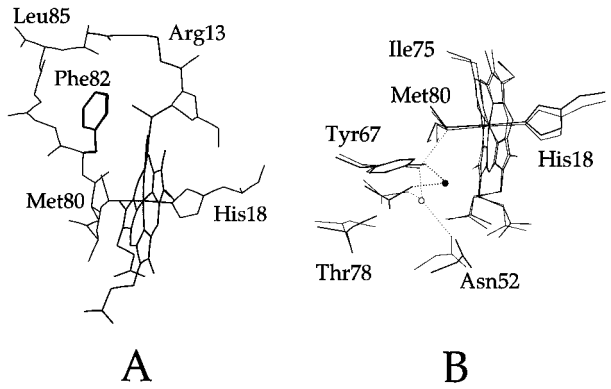

FIGURE 1: (A) Environment of the invariant residue Phe82 in wild-type yeast iso-1-ferrocytochrome *c* (Louie & Brayer, 1990). (B) The oxidation state-linked conformational changes around Wat166 in yeast iso-1-cytochrome *c* (Louie & Brayer, 1990; Berghuis & Brayer, 1992): thin lines, reduced; thick lines, oxidized. The dashed lines represent hydrogen bonds to Wat166, which is represented by the circles (open, reduced; solid, oxidized).

the exposed heme edge that modulates the distance between donor and acceptor sites (Louie et al., 1988; Louie & Brayer, 1989; Rafferty et al., 1990).

A second region of interest not previously addressed systematically is the internal hydrogen bond network consisting of conserved residues Thr78, Tyr67, Asn52, and a buried water molecule (Wat166). This network is the site of the largest conformational differences between oxidized and reduced cytochrome *c* (Takano & Dickerson, 1981a,b; Berghuis & Brayer, 1992) (Figure 1B). Upon oxidation of yeast iso-1-cytochrome *c*, Wat166 moves 1.7 Å toward the heme. This movement is consistent with stabilization of the positive charge on the oxidized heme by the buried solvent molecule. This region also includes the conserved residue Ile75, which, although not part of the hydrogen bond network, shields this region from exposure to the solvent.

In the present study, we extend our initial work on the electron transfer reactivity of cytochrome *c* variants toward inorganic complexes through consideration of the kinetics of both reduction and oxidation of two series of variants and correlating the results with corresponding electrochemical measurements. Specifically, the reactivities of position-82 variants toward the oxidant $Co(phen)_3^{3+}$ have been studied to complement our previous analysis of reduction kinetics involving $Fe(EDTA)^{2-}$. In addition, the electron transfer reactivities of variants modified in the region involving the hydrogen-bonding network around Wat166 toward both $Fe(EDTA)^{2-}$ and $Co(phen)_3^{3+}$ have been determined. These results combined with three-dimensional structures reported here for the Asn52Ala and Ile75Met variants provide mechanistic insight into the different functional roles played by these two regions of the protein in electron transfer and demonstrate the sensitivity of cytochrome *c* reactivity to both surface modifications and internal alterations remote from the contact surface with which electron transfer reagents interact.

EXPERIMENTAL PROCEDURES

Site-directed mutagenesis (Pielak et al., 1985; Inglis et al., 1991), protein expression and purification (Rafferty et al., 1990), and direct electrochemical measurements (Rafferty et al., 1990) of yeast iso-1-cytochrome *c* were performed as described previously. Kinetic experiments were performed with a Durrum Model D-110 stopped flow spectrophotometer interfaced to a microcomputer (OLIS, Bogart, GA) and modified as described previously to improve anaerobicity (Reid & Mauk, 1982; Reid, 1984). The new variants constructed in this work were those involving internally located residues: Tyr67Phe, Asn52Ala, Thr78Gly, and Ile75Met. All variants also possessed the Cys102Thr substitution to eliminate complications arising from the reactive cysteine residue of the wild-type protein (Cutler et al., 1987).

Protein Crystallization and X-Ray Diffraction Data Collection. Crystals of the reduced [Fe(II)] Asn52Ala variant were initially grown in 0.1 M sodium phosphate buffer (pH 6.4) containing 90% saturated ammonium sulfate and 60 mM DTT using a combination of the hanging drop method and a hair-seeding technique (Leung et al., 1989). The crystals produced by this method were of insufficient size for high-resolution X-ray diffraction analyses, so macroseeding was employed to produce larger crystals. The Fe(II)−Ile75Met variant was crystallized similarly in 0.1 M sodium phosphate buffer (pH 5.3) containing 95% saturated ammonium sulfate and 70 mM sodium dithionite. Prior to mounting for collection of X-ray diffraction data, crystals were transferred to fresh mother liquor, which in the case of Ile75Met contained 40 mM DTT instead of sodium dithionite. Crystals of the variant proteins were of the space group $P4_32_12$ and were isomorphous with those of wild-type yeast iso-1-cytochrome *c*. Cell dimensions for the wild-type and variant protein crystals were as follows: Asn52Ala, $a = b = 36.52$ Å, $c = 137.89$ Å; Ile75Met, $a = b = 36.55$ Å, $c = 138.59$ Å; and wild-type, $a = b = 36.46$ Å, $c = 136.86$ Å.

Diffraction data for the Asn52Ala and Ile75Met variants were collected from a single crystal of each with an Enraf-Nonius CAD4-F11 diffractometer equipped with a helium beam path and operated at 26 mA and 40 kV. The incident radiation was generated from a Cu sealed beam tube and Ni filtered. To monitor slippage and decay, six reflections were measured periodically. A total of 10 779 reflections (6852 unique) were collected to a resolution of 2.0 Å for the Asn52Ala variant, and 10 308 reflections (7722 unique) were collected to a resolution of 1.9 Å for the Ile75Met variant. For the resolution ranges used, a total of 100 and 95% of the potentially available diffraction data was collected for the Asn52Ala and Ile75Met variants, respectively. Diffraction intensities were corrected for background, absorption, decay, Lorentz, and polarization effects as previously described (Berghuis & Brayer, 1992). Structure factors for both variant proteins were put on an absolute scale using the Wilson plot method (Wilson, 1942).

Synthesis of $[Co(phen)_3]Cl_3$. *o*-Phenanthroline monohydrate (BDH, 4.0 g, 0.02 mol) and 60 mL of water were placed in a modified three-necked 300 mL round bottom flask. $CoCl_2 \cdot 6H_2O$ (MCB, 1.6 g, 0.0067 mol) was dissolved in 60 mL of water; this solution was added incrementally with a Pasteur pipette to the phenanthroline suspension with swirling of the flask. During the addition of the $CoCl_2$, the contents of the flask turned brown, and the phenanthroline dissolved completely. The resulting solution was heated briefly on a steam bath and cooled to room temperature. The Co(II) complex was oxidized with chlorine gas generated by potassium permanganate oxidation of hydrochloric acid as described by Vogel (1978). The solution containing the oxidized product was heated with stirring on a hot plate until

the volume was reduced to ~20 mL. The resulting solution was diluted to 60 mL with water, and the volume was reduced as before; this procedure was repeated twice. The precipitated product was recrystallized from 95% ethanol, washed with diethyl ether, and air-dried. The reduction potential of $Co(phen)_3^{3+/2+}$ was determined by cyclic voltammetry at a gold electrode to be 370 mV (pH 6, $\mu = 0.1$ M, and 25 °C), in agreement with previous spectroelectrochemical measurements under similar conditions [377 mV (Taniguchi et al., 1982)]. The extinction coefficients of the $Co(phen)_3Cl_3$ product at 330 (4700 M^{-1} cm^{-1}) and 350 nm (3730 M^{-1} cm^{-1}) agreed with those (4680 and 3700 M^{-1} cm^{-1}, respectively) reported previously (Przystas & Sutin, 1973).

Ferrocytochrome c Oxidation by $Co(phen)_3Cl_3$. Buffered $Co(phen)_3Cl_3$ solutions [$\mu = 0.1$ M (2 mM MES, balance NaCl) and pH 6.0] were stored in modified three-necked 100 mL round bottom flasks equipped with Luer fittings. Buffered ferrocytochrome *c* solutions (10−20 μM) were prepared on the day of use by reduction with dithionite followed immediately by gel filtration (Bio-Rad P6-DG, 1 × 10 cm column equilibrated with deaerated buffer) to remove residual reductant. The reduced cytochrome solution was collected in a serum bottle, diluted with deaerated buffer to a concentration of 10−20 μM, and kept under a water-saturated argon atmosphere. Oxidation of cytochrome *c* by $Co(phen)_3Cl_3$ was monitored at 550 nm under pseudo-first-order conditions with oxidant in an at least 10-fold excess and at seven different concentrations (0.2−1.6 mM).

Ferricytochrome c Reduction by $Fe(EDTA)^{2-}$. $Fe(EDTA)^{2-}$ solutions were prepared anaerobically on the day of use in phosphate buffer as described by Wherland et al. (1975). Buffered ferricytochrome *c* (5 μM) solutions were deaerated by a stream of water-saturated, purified argon. The reduction of cytochrome *c* by $Fe(EDTA)^{2-}$ was monitored at 412.5 nm under pseudo-first-order conditions with the reductant concentration in an at least 10-fold excess ($\mu = 0.1$ M, sodium phosphate buffer, pH 6.0, and 25.0 °C) and at six different concentrations (0.05−0.5 mM).

Direct Electrochemistry. Midpoint reduction potentials of the variants with substitutions near Wat166 were determined by direct electrochemistry [$\mu = 0.1$ M, pH 6.0 (50 mM in KCl with the balance of the ionic strength provided by sodium phosphate buffer), and 25 °C] at a gold electrode surface modified with 4,4′-dithiodipyridine (Aldrich) using the electrochemical cell, potentiostat, and thermostatted water bath used previously for related studies of the position-82 variants (Rafferty et al., 1990; Rafferty, 1992). Potentials were measured relative to a saturated calomel reference electrode (Radiometer Model K401) and converted to the hydrogen scale as described by Dutton (1978).

RESULTS

X-ray Diffraction Analyses. Variant minus wild-type difference Fourier maps revealed that neither the Asn52Ala nor the Ile75Met variant differed in structure from wild-type cytochrome *c* except for the regions directly surrounding the mutation sites. Least-squares restrained parameter refinement (Hendrickson & Konnert, 1981) was, therefore, initiated for both cytochrome variants using the wild-type yeast iso-1-cytochrome *c* structure (Louie & Brayer, 1990) in which the modified residues were replaced by alanine to produce initial models. A number of well-determined solvent molecules other than Wat166, which is located adjacent to the side chains of residues 52 and 75, were also included in the starting models. Structural refinement used diffraction data from 6.0 to 2.0/1.9 Å resolution with a cutoff of $F/\sigma_F > 2.0$ and included 4416 and 3645 reflections for the Asn52Ala and Ile75Met variants, respectively. Several manual interventions were executed during the refinement process. On the basis of the inspection of $F_o - F_c$, $2F_o - F_c$, and $3F_o - 2F_c$ difference electron density maps, the solvent structure and surface side chains with high degrees of mobility were adjusted in both structures, and the remaining side chain atoms of Met75 were added to the Ile75Met structure. The crystallographic *R*-factors for the two structures indicate that the final models for both variants agree well with the experimental data (18.5% for Asn52Ala and 22.1% for Ile75Met). As shown in Table 1, both structures display nearly ideal stereochemistry. The accuracy of the two structures was assessed with Luzzati plots (Luzzati, 1952), and these indicated an overall rms coordinate error of ~0.20 Å for the Asn52Ala structure and ~0.24 Å for the Ile75Met structure. The difference in estimated coordinate error for these two structures most likely results from the smaller and poorer quality of the crystals grown for the Ile75Met protein.

Table 1: Final Stereochemistry for the Asn52Ala and Ile75Met Yeast Iso-1-ferrocytochrome *c* Variants

stereochemical refinement parameters	rms deviation from ideal values	
	Asn52Ala	Ile75Met
bond distances (Å)		
1−2 bond distance	0.020	0.024
1−3 bond distance	0.044	0.050
1−4 bond distance	0.052	0.064
planar restraints (Å)	0.016	0.018
chiral volume (Å^3)	0.196	0.286
nonbonded contacts[a] (Å)		
single-torsion	0.219	0.236
multi-torsion	0.207	0.242
possible hydrogen bonds	0.245	0.262
torsion angles (degrees)		
planar (0 or 180°)	2.6	2.6
staggered (±60°, 180°)	25.9	26.3

[a] The rms deviations from ideality for this class of restraint incorporates a reduction of 0.2 Å from the radius of each atom involved in a contact.

As seen in Figure 2, the substitutions at positions 52 and 75 do not affect the overall polypeptide fold of cytochrome *c* despite the internal locations of these residues. Nonetheless, two regions display displacements that differ by more than twice the average deviation in the two structures: the amino terminus and the region around Gly41 (and the pyrrole A propionate). The former region is disordered in all yeast iso-1-cytochrome *c* structures determined thus far (Louie et al., 1988; Louie & Brayer, 1989; Berghuis & Brayer, 1992), and therefore, the differences observed arise from alternative structural fits in this region to the poorly defined electron density available. The changes occurring in the vicinity of the propionate on pyrrole A merit detailed description for each of the two variant structures determined here.

The replacement of Asn52 with Ala results in the introduction of a water molecule (Wat300) into the protein where the Asn52 ND2 group is located in the wild-type protein (Figure 3a). The thermal factor for this water molecule is high (50 Å^2) and indicates that this water

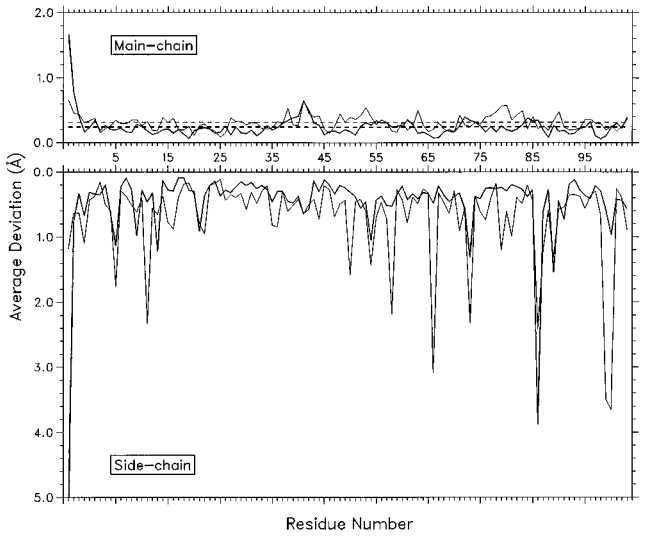

FIGURE 2: Average positional deviations between the Asn52Ala (thick lines) and Ile75Met (thin lines) variants and the wild-type structure of yeast iso-1-cytochrome *c*. The top frame shows the observed deviations for main chain atoms, while the bottom frame displays the deviations observed for side chain atoms. The dashed lines in the top frame represent the overall average deviations of all main chain atoms for the two variants that are 0.24 and 0.31 Å for the Asn52Ala and Ile75Met structures, respectively.

molecule is highly mobile. This mobility combined with the distance between Wat300 and the heme propionate O2A oxygen (3.6 Å) suggests that a hydrogen bond between these groups is at best transient. The hydrogen bond network around the pyrrole A propionate is further altered in the Asn52Ala variant by the strengthening of its interaction with Gly41 N. Movement of Gly41 toward the propionate group reduces the length of the hydrogen bond between these two groups by 0.5 Å to a distance of 2.7 Å. Hydrogen-bonding interactions in this region of both variant proteins are defined in detail in Table 2.

In the Ile75Met variant, the torsion angles of the propionate A group have each rotated ∼20−25° (Figure 3b). This conformational change shifts the heme O1A and O2A atoms 0.3 and 0.5 Å toward Arg38, respectively, a movement reminiscent of the change that occurs in this region of the wild-type protein with oxidation of the heme iron (Berghuis & Brayer, 1992). Concomitant with this shift, the Asn52 ND2 atom shifts away from this propionate group toward the substituted residue Met75. This movement increases the distance between the Asn ND2 to heme O2A atoms from 3.34 to 4.15 Å and breaks the hydrogen bond formed between these two groups in the wild-type protein. As observed in the Asn52Ala structure, the loss of this hydrogen bond results in a strengthened interaction between Gly41 N and the heme O2A atom, with residue 41 moving toward the propionate to decrease the distance between these two groups from 3.2 to 2.6 Å (Table 2).

Both variants also exhibit a saddle-like distortion of the heme prosthetic group from planarity as observed to occur previously for the Tyr67Phe (Berghuis et al., 1994a) and Asn52Ile (Berghuis et al., 1994b) variants. For the Asn52Ala and Ile75Met variants, the average angular deviations between the pyrrole N plane normal and the four pyrrole ring plane normals are 11.8 and 13.6°, respectively. Finally, the overall effects of these two mutations on the structure of ferrocytochrome *c* are summarized in Table 3.

Electrochemical Measurements. The direct electrochemistry of the cytochrome *c* variants was quasi-reversible as indicated by peak to peak separations of 54−63 mV (25 °C, 20 mV s^{-1} scan rate) obtained from the majority of the voltammograms. The dependence of the Faradaic current on the square root of the scan rate was measured for several proteins and was found to be linear up to 50 mV s^{-1}. The midpoint reduction potentials for the variants modified in the vicinity of Wat166 are shown in Table 4.

Oxidation of Cytochrome c Variants by $Co(phen)_3Cl_3$. For each cytochrome *c* variant, the dependence of the observed reaction rate on oxidant concentration was linear. The intercept of each plot was within experimental error of zero. Second-order rate constants were determined by fitting the dependence of the observed rate constant on reagent concentration by the method of least squares. The resulting second-order rate constants are displayed in Table 5.

To account for differences in thermodynamic driving force on the observed reaction rates, apparent self-exchange rate constants calculated for these reactions, k_{11}^{corr}, were determined as described by Wherland and Gray (1976, 1977). These values are also presented in Table 5. For most position-82 variants, the differences in k_{11}^{corr} span only a 3-fold range and show a small dependence on the size of the side chain at this position. One exception to this general relationship is the Phe82Ile variant, with a k_{11}^{corr} almost 7-fold greater than that of wild type. The reactivities of the Wat166-related variants toward $Co(phen)_3^{3+}$ are up to 11-fold greater than that of wild type; none is less reactive than the wild-type protein.

Reduction of Cytochrome c Variants by $Fe(EDTA)^{2-}$. As for the oxidation rate constants, the observed rates of variant cytochrome *c* reduction were linearly dependent on reductant concentration over the range of reactant concentrations examined, and the second-order rate constants were determined as above (Table 6). On the basis of calculations of electrostatics-corrected apparent self-exchange rates by relative Marcus theory, the Phe82Gly and Phe82Ser variants possess the highest reactivity, with k_{11}^{corr} values of 165 and 190 M^{-1} s^{-1}, respectively. The variants modified at internally located residues exhibit k_{11}^{corr} values in the same range observed for oxidation by $Co(phen)_3^{3+}$.

DISCUSSION

Interpretation of the electrochemical and kinetic results obtained for the cytochrome *c* variants studied in this investigation requires consideration of several structural and functional characteristics of the proteins and the small molecule reagents involved, and the contributions of these characteristics to the rate constants are summarized in Tables 5 and 6. The characteristics of primary concern in this analysis include the effects of the mutations on the structure of cytochrome *c* and the electrochemical and electrostatic properties of the cytochromes and small molecule reagents involved. The functional properties required for this analysis are provided by the present work. A substantial portion of the structural information required is provided in the current study and by previous crystallographic studies (Louie et al., 1988; Louie & Brayer, 1990; Berghuis & Brayer, 1992).

Interpretation of Kinetic Results. The most thoroughly documented strategy for correlating these factors involves the use of relative Marcus theory as developed by the work

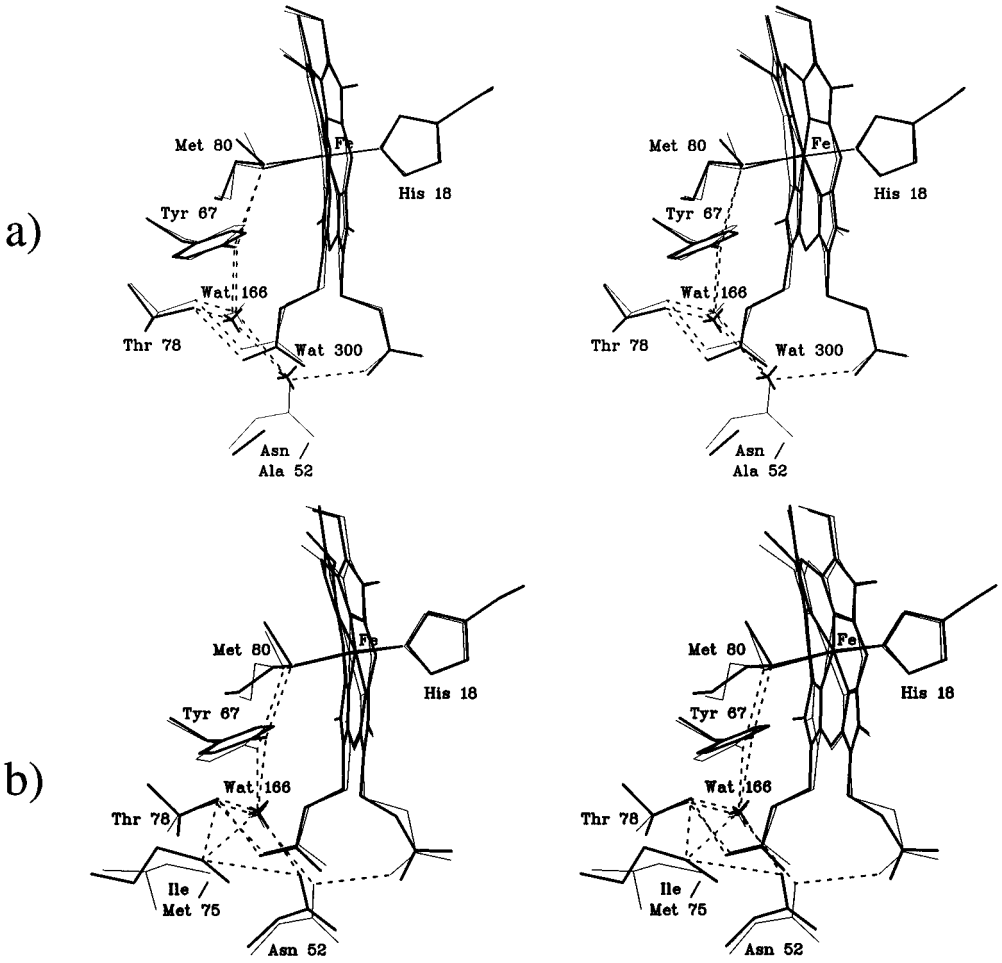

FIGURE 3: (a) Stereochemical drawing of the region near residue 52 in the Asn52Ala (thick lines) and wild-type (thin lines) yeast iso-1-cytochromes *c*. This substitution substantially increases the volume of an internal water cavity and leads to the inclusion of an additional water molecule (Wat300). The hydrogen bonds (dashed lines) formed by Wat300 are similar to those formed by Asn52 ND2 in the wild-type structure. (b) Stereochemical drawing of the region near residue 75 in the Ile75Met variant (thick lines) and wild-type (thin lines) yeast iso-1-cytochromes *c*. The presence of the Met75 SD sulfur atom adds another group to the hydrogen bond network (dashed lines) around Wat166.

Table 2: Heme Propionate Hydrogen Bond Interactions in Wild-Type Yeast Iso-1-ferrocytochrome *c* and the Asn52Ala and Ile75Met Variants

hydrogen bond partners[a]		distances (Å)		
		wild-type	Asn52Ala	Ile75Met
O1A	Tyr48 OH	2.83	2.89	2.82
	Wat121	2.81	2.97	3.37
	Wat168	2.85	3.24	3.03
O2A	Gly41 N	3.21	2.69	2.63
	Asn52 ND2	3.34	(3.56)[b]	(4.15)
	Trp59 NE1	3.09	2.82	3.04
O1D	Thr49 OG1	2.64	2.44	2.79
	Thr78 OG1	2.90	3.16	2.97
	Lys79 N	3.17	3.14	2.90
O2D	Thr49 N	2.94	2.74	2.55

[a] Interactions were regarded as hydrogen bonds only if they met all of the following criteria: a H−A distance of <2.6 Å, a D−H−A angle of >120°, and a C−A−H angle of >90°. Values in parentheses are not considered to be hydrogen bonds by these criteria but are listed for comparison. [b] This value refers to the distance between heme O2A and Wat300.

of Gray and colleagues in their extensive kinetic studies of small molecule oxidation and reduction of simple metalloproteins (Wherland & Gray, 1976, 1977). The advantage provided by this strategy is that it permits correction of the second-order rate constants determined experimentally for the contributions resulting from the thermodynamic driving force of the reaction (i.e., the difference in reduction potentials of the protein and the reagent in question), the electrostatic attraction of the protein and reagent for each other (as approximated by Debye−Hückel theory), and the intrinsic reactivity of the small molecule reagent in electron transfer reactions (as reflected by the self-exchange rate of this reagent). As employed by Gray and co-workers, the self-exchange rate constant demonstrated by a protein (k_{11}) in its reaction with a redox-active reagent is a function of the self-exchange rate of the reagent (k_{22}) and the thermodynamic driving force for the reaction ($\Delta E°$) as defined by relative Marcus theory (Marcus & Sutin, 1974; Wherland & Gray, 1976, 1977) in the following relationship: $k_{12} = (k_{11}k_{22}Kf)^{1/2}$. In this expression, the factor f is near unity for reactions with small equilibrium constants as in the current study.

The electrostatics contribution to the experimentally determined second-order rate constant used in this calculation can be accounted for by first correcting the second-order rate constant for the electrostatics work terms for association of the protein−reagent precursor complex and for dissociation of the protein−reagent successor complex through use of Debye−Hückel theory as described by Wherland and Gray (1976, 1977). With this additional consideration, the ap-

Table 3: Structural Differences Observed in the Asn52Ala and Ile75Met Variant Structures Relative to That of Wild-Type Yeast Iso-1-ferrocytochrome *c*

Asn52Ala	Ile75Met
(A) Positional Displacements of Polypeptide Chain	
Gly41 moves toward pyrrole A propionate	Gly41 moves toward pyrrole A propionate
(B) Thermal Factor Parameters of Main Chain Atoms	
thermal factor profile similar to that observed for wild-type ferrocytochrome	increased thermal factors for residues 42−46 and 57−59
(C) Heme Structure	
(1) heme plane more distorted (similar to ferricytochrome *c*)	(1) heme plane more distorted (similar to ferricytochrome *c*)
(2) small readjustment to pyrrole A propionate	(2) propionate conformation similar to that observed in wild-type ferricytochrome
(D) Mutation Site	
(1) new water molecule (Wat300) occupies space that Asn52 ND2 occupies in wild-type structure	(1) addition of an extra hydrogen bond acceptor group in the Wat166 hydrogen bond network
	(2) shift of Asn52 side chain toward Met75 and away from the pyrrole A propionate
(E) Hydrogen Bond Interactions	
stronger: Gly41 N−heme O2A	stronger: Gly41 N−heme O2A
lost: Asn52 ND2−heme O2A	weaker: Wat121−heme O1A
Asn52 ND2−Wat166	lost: Asn52 ND2−heme O2A
new: Wat300−Wat166	new: Met75 SD−Asn52 ND2
	Met75 SD−Thr78 OG1
	Met75 SD−Wat166

Table 4: Reduction Potentials of Cytochrome *c* Variants Determined by Direct Electrochemistry[a]

protein	$E°$ (vs SHE) (mV)
wild-type[b]	290
Phe82Tyr[b]	280
Phe82Leu[b]	286
Phe82Ile[b]	273
Phe82Ser[b]	255
Phe82Gly[b]	247
Asn52Ala[c]	257
Tyr67Phe[c]	236
Ile75Met[c]	249
Thr78Gly[c]	245

[a] pH 6.0, μ = 0.1 M, and 25 °C. [b] Rafferty et al. (1990). [c] This work.

Table 5: Rate Constants for Oxidation of Ferrocytochrome *c* Variants by $Co(phen)_3^{3+}$ [a]

protein	rate constant $(M^{-1}\,s^{-1})$[b]	k_{11}^{corr} $(M^{-1}\,s^{-1})$[c]	relative k_{11}^{corr}
wild-type	1.7×10^3	3.1×10^3	1.0
Phe82Tyr	2.4×10^3	4.1×10^3	1.3
Phe82Leu	2.4×10^3	5.0×10^3	1.6
Phe82Ile	6.1×10^3	2.1×10^4	6.8
Phe82Ser	5.4×10^3	8.1×10^3	2.6
Phe82Gly	6.6×10^3	9.2×10^3	3.0
Thr78Gly	5.6×10^3	7.0×10^3	2.3
Ile75Met	4.1×10^3	3.2×10^3	1.0
Asn52Ala	6.2×10^3	1.1×10^4	3.5
Tyr67Phe	1.5×10^4	3.3×10^4	10.6

[a] pH 6.0, μ = 0.1 M (2 mM MES and 98 mM NaCl), and 25 °C. [b] The uncertainties in the rate constants are ∼5%. [c] The following parameters were used: $E_{m,6}$ = 370 mV, k_{22} = 41.7 $M^{-1}\,s^{-1}$ (Baker *et al.*, 1959), radius = 7 Å (Wherland & Gray, 1976a), and charge = +3 (oxidized) or +2 (reduced). Cytochrome *c*: radius = 16.7 Å and charge = +7 (oxidized) or +6 (reduced).

parent electrostatics-corrected self-exchange rate exhibited by the protein in its reaction with the redox reagent (k_{11}^{corr}) can be determined. For electron transfer reactions involving one substitutionally inert, small molecule reactant (A) with a wide range of similar reagents (B), the self-exchange rates (k_{11}) determined in this manner for A usually are within 1 order of magnitude of each other (Wherland & Gray, 1976, 1977). When A is an electron transfer protein, the values of k_{11} (or k_{11}^{corr}) determined in this manner can vary over several orders of magnitude.

Table 6: Rate Constants for Reduction of Ferricytochrome *c* Variants by $Fe(EDTA)^{2-}$ [a]

protein	rate constant $(M^{-1}\,s^{-1})$[b]	k_{11}^{corr} $(M^{-1}\,s^{-1})$[c]	relative k_{11}^{corr}
wild-type[d]	7.2×10^4	10.9	1.0
Phe82Tyr[d]	6.2×10^4	11.8	1.1
Phe82Leu[d]	8.8×10^4	19	1.7
Phe82Ile[d]	9.4×10^4	35	3.2
Phe82Ala[d]	9.9×10^4	62	5.7
Phe82Ser[d]	1.48×10^5	165	15.1
Phe82Gly[d]	1.37×10^5	190	17.4
Thr78Gly	5.9×10^4	33.5	3.1
Ile75Met	4.2×10^4	19	1.7
Asn52Ala	8.9×10^4	56	5.1
Tyr67Phe	8.8×10^4	119	10.9

[a] pH 6.0, μ = 0.1 M (sodium phosphate), and 25 °C. [b] The uncertainty in the second-order rate constants is ∼5%. [c] The following parameters were used: $Fe(EDTA)^{2-}$, $E_{m,6}$ = 104 mV (Reid, 1984), k_{22} = 3×10^4 $M^{-1}\,s^{-1}$ (Wilkins & Yelin, 1968), radius = 4 Å (Wherland & Gray, 1976a), and charge = −1 (oxidized) or −2 (reduced); other parameters were as in Table 5. [d] Rafferty et al. (1990).

This variation has been interpreted as arising from specific interactions between the protein and the small reagent that are not accounted for by Marcus theory (Wherland & Gray, 1976, 1977). As a result, consideration of k_{11}^{corr} values provides mechanistic information devoid of the contributions outlined above that can provide insight into the mechanism employed by a protein or a family of proteins in their reactions with small reagents. As the proteins and small molecule reactants used here vary in their reduction potentials and electrostatic properties, the ability to eliminate these contributions from the experimentally determined second-order rate constants permits interpretation of the effects of our mutations on the mechanism of electron transfer used by these proteins in the reactions studied in this work.

On the basis of this formalism, it is possible to discuss the mechanistic origins of the differences in oxidation and

reduction rates observed for the cytochrome *c* variants studied here. Before undertaking this analysis, however, we first consider the mechanistic origins of the changes in midpoint reduction potentials caused by the amino acid substitutions around Wat166. The corresponding analysis of the electrochemical effects of substitutions at position-82 has been presented elsewhere (Rafferty et al., 1990).

Electrochemical Consequences of Substitutions around Wat166. Replacement of internal residues such as those represented in this family of variants raises concern regarding the effects of our substitutions on the overall structure of cytochrome *c*. Attempts to prepare crystals of the Thr78Gly protein have so far been unsuccessful, so detailed structural knowledge of this protein is not available. However, in previous studies, structural information concerning the Tyr67Phe (Berghuis et al., 1994a) and Asn52Ile variants in both oxidation states (Berghuis et al., 1994b) has been reported. The structures of both of these variants and the two new structures reported here establish that amino acid substitutions in this region of the protein allow retention of polypeptide chain conformation and axial ligation that are characteristic of the wild-type protein. Furthermore, the apparent lack of significant structural rearrangement combined with the electrostatically neutral nature of the wild-type and variant residues at the positions concerned argue that the electrostatic properties of the proteins studied here are essentially identical to those of the wild-type protein for the purposes of our analysis.

We note that the effects of the substitutions studied in the current work on the pK_a of the alkaline conformation change are minimal, except in the case of the Thr78Gly variant (pK_{alk} $\sim$ 7; J. G. Guillemette, unpublished). Nevertheless, the contribution of this effect has been minimized in the present work by conducting most experiments at pH 6.0, which is sufficiently low to minimize contributions from alkaline ferricytochrome *c*. Moreover, reduction of alkaline cytochrome *c* occurs at a sufficiently slow rate (Barker & Mauk, 1992) that it should not contribute to our current observations, whereas reduced alkaline cytochrome *c* is only transiently stable and does not contribute to the oxidation kinetics (Barker & Mauk, 1992). Therefore, the variations in electron transfer reactivity observed for the proteins in the present study may be reasonably interpreted in terms of the effects of these substitutions on the relative stabilities of the native reduced and oxidized states of these proteins (electrochemical effects) and on the mechanisms by which these proteins change oxidation state (kinetic effects).

The substitutions in the vicinity of Wat166 studied here all decrease the reduction potential of cytochrome *c*. From the three-dimensional structures determined in this work, it is apparent that the dielectric of the heme environment and the axial ligation of the heme iron are unaffected by replacement of Asn52 by Ala or the replacement of Ile75 by Met. To explain the effects of these substitutions on the oxidation−reduction equilibrium of this protein, therefore, it is necessary to consider their effects on the hydrogen-bonding interactions of Wat166 in greater detail. In the wild-type protein, the Asn52 ND2 atom functions as a hydrogen bond donor to Wat166 (Figure 3). In the Asn52Ala variant, this role of the ND2 atom is assumed by the new water molecule Wat300. A water molecule, however, can donate or accept a hydrogen bond from Wat166, effectively reducing the hydrogen bond donor capacity and increasing the hydrogen bond acceptor capacity on the side of the Wat166 molecule away from Tyr67. The replacement of Ile75 with a Met residue has a similar effect in that it also increases the hydrogen bond acceptor capacity on the side of Wat166 that is away from Tyr67. This result occurs despite the poor hydrogen bond-accepting capacity of methionine sulfur atoms. In both of these variants, therefore, the orientation of Wat166 is modified from that of Wat166 in the wild-type protein.

The orientation of Wat166 has been proposed to be a determinant of the relative stabilities of reduced and oxidized cytochrome *c* (Berghuis & Brayer, 1992). In ferrocytochrome *c*, Wat166 is oriented to maximize the number of hydrogen bonds that it can form (Figure 3). In ferricytochrome *c*, however, Wat166 reorients so that its dipole moment can interact optimally with the net positive charge resident on the heme iron. As a result of this reorientation, the hydrogen bond between the phenolic hydroxyl oxygen of Tyr67 and the sulfur atom of Met80 is broken in ferricytochrome *c*. The loss of this hydrogen bond stabilizes ferricytochrome *c* because the lone-pair electrons of the Met80 SD atom are better able to interact with the charge on the heme iron. In both the Asn52Ala and Ile75Met variants, Wat166 of the ferrocytochrome will tend to serve as a hydrogen bond donor to Wat300 or the Met75 SD atom, respectively. Similarly, in each of these variants, the Tyr67 hydroxyl group will tend to serve as a hydrogen bond donor to Wat166 and the interaction of the hydroxyl group with the Met80 SD atom will be weakened. As a result, the structures of the reduced variants are more similar to that of the ferricytochrome than that seen for the wild-type ferrocytochrome.

This proposal would also be consistent with the finding that the reduction potential of the Thr78Gly variant (247 mV) is similar to that of the Asn52Ala and Ile75Met variants. In the Thr78Gly variant, it is likely that a second water molecule replaces the hydrogen-bonding hydroxyl group of the Thr78 residue. However, one must also consider that in this variant the entire branched side chain of the threonine residue would not be present. Therefore, an alternative explanation in the absence of structural data is that the polypeptide backbone in the region of the mutation folds in a manner different from that of the wild-type protein to avoid the formation of a large cavity and that this leads to a decrease in reduction potential.

Electron Transfer Reactivity. If the mechanisms by which the cytochrome variants studied here are reduced by $Fe(EDTA)^{2-}$ and oxidized by $Co(phen)_3^{3+}$ are identical, then a plot of k_{11}^{corr} for the reduction reaction vs k_{11}^{corr} for the oxidation reaction should be a straight line. Examination of Figure 4, in which this correlation is evaluated, demonstrates that the cytochrome variants near Wat166 exhibit this type of behavior. In other words, the electron transfer reactivity of these variants is independent of the nature of the small molecule reagent with which they react. On the other hand, the variants in which Phe82 is replaced demonstrate variable behavior, which presumably results from the position of this residue on the surface of the protein. In the following discussion, we first consider the structural origins of this electron transfer reactivity for the variants in the vicinity of Wat166 and then consider the structural basis for the behavior of the position-82 variants.

Cytochrome c Variants Modified Near Wat166. The reactivity exhibited by the variants modified in the vicinity

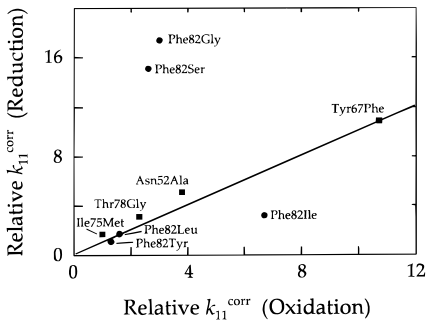

FIGURE 4: Comparison of the relative self-exchange rates obtained for the reactions of the variant cytochromes with $Fe(EDTA)^{2-}$ (ordinate) and $Co(phen)_3^{3+}$ (abscissa). The line corresponds to equal values for the two relative self-exchange rates.

of Wat166 toward $Fe(EDTA)^{2-}$ and $Co(phen)_3^{3+}$ demonstrates that the specific arrangement of the hydrogen bond network in the region of the mutated residues is not a prerequisite for rapid electron transfer. In both the Tyr67Phe and Asn52Ala variants, replacement of a hydrogen-bonding side chain by a second buried water molecule results in an increase in electron transfer reactivity. When the cross-reaction rates and the reduction potentials are used with the relative Marcus equation to calculate the self-exchange rate constant for each protein, one finds that Tyr67Phe is 11 times more reactive than the wild-type cytochrome toward both electron transfer partners.

The electron transfer reactivities of the Wat166 variants relative to the wild-type protein show little dependence on the identity of their electron transfer partners. This observation suggests that these substitutions do not influence the interaction surface of the protein as do the position-82 variants. Rather, the differences in reactivity that are observed with these variants are caused by adjustments in the reorganization energy of the protein. The lower reorganization energies of the Tyr67Phe, Asn52Ala, and possibly the Thr78Gly variants may be caused by smaller movements in the protein surrounding the heme and greater movement of the internal water molecules. In wild-type cytochrome *c*, reorganization in the hydrogen bond network around Wat166 requires movement of hydrogen-bonding side chains that are held in place by the protein backbone. In Tyr67Phe, Asn52Ala, and possibly Thr78Gly, the second internal water molecule should have more freedom to move than the hydrogen-bonding side chain that it replaces. Reorganization may simply involve facile movement of internal water molecules rather than movement of somewhat constrained side chain residues. Internal water molecules closest to the heme would be expected to have the largest effect, which would diminish as their distance from the heme increases. This possibility would explain the order of reactivity of the three internal site variants with additional internal water molecules (Table 5).

The electron transfer properties of the variants affecting the region around Wat166 suggest that one of the roles of the hydrogen bond network in this region is to lower the reorganization energy of cytochrome *c* by promoting movement of this internal solvent molecule so that movement of the surrounding polypeptide is minimized. The structure of another related variant of this cytochrome, Asn52Ile, has been reported (Hickey et al., 1991). This protein completely lacks internal solvent molecules, including Wat166. Despite the absence of internal water molecules, this variant appears to be functional and considerably more thermodynamically stable than the wild-type protein. Electron transfer kinetics of Asn52Ile with inorganic complexes have not yet been reported. The absence of internal water molecules requires that the reorganization energy of Ile52 prior to electron transfer results solely from movement of the polypeptide chain in the vicinity of the heme. If this is the case, then the present results suggest that the reactivity of Asn52Ile may be lower than those of Tyr67Phe, Asn52Ala, and Thr78Gly. On the other hand, the absence of Wat166 in the Asn52Ile variant results in greater flexibility for Tyr67, as indicated by formation of a new H bond with Thr78 in this variant, which could reduce the requirement for oxidation-state dependent polypeptide rearrangement in the Asn52Ile variant to preserve facile electron transfer reactivity.

Cytochrome c Variants with Substitutions at Position-82. The analysis of the oxidation of this family of variants by $Co(phen)_3^{3+}$ complements our previous investigation of the reduction of these proteins by $Fe(EDTA)^{2-}$ (Rafferty et al., 1990). We interpret the principal influence of mutations at position-82 on the reactivity of cytochrome *c* as arising from the nature of the precursor complex formed between cytochrome *c* and its electron transfer partners. As the size of the residue at position-82 decreases, reactivity increases. This affect is probably attributable to shorter distances between electron transfer centers, with position-82 variants having small side chains allowing the electron transfer partner to approach the heme more closely. This trend is seen clearly with the results of kinetics experiments using $Fe(EDTA)^{2-}$, where k_{11}^{corr} varies over a 17-fold range. With oxidation of ferrocytochrome *c* by $Co(phen)_3^{3+}$, the trend is the same, but it is less pronounced; the reactivity varies only over a 7-fold range. The greatest sensitivity toward the identity of the electron transfer partner occurs with Phe82Gly and Phe82Ser which are 15−17 times more reactive than wild-type cytochrome *c* toward $Fe(EDTA)^{2-}$ but only 2.6−3 times more reactive toward $Co(phen)_3^{3+}$. This behavior of these two variants is reflected in their failure to comply with the linear correlation indicated in Figure 4.

In addition to altering the nature of the precursor complex by decreasing the distance between the electron donor and acceptor centers, Phe82Gly and Phe82Ser may increase reactivity by decreasing the reorganization energy of cytochrome *c*. In the structures of both of these ferrocytochrome variants, Wat166 is ∼1 Å closer to the heme than it is in the wild-type protein, giving the reduced structure some characteristics of the oxidized structure (Louie et al., 1988; Louie & Brayer, 1989). Although most position-82 variants are more reactive toward $Fe(EDTA)^{2-}$ than towards $Co(phen)_3^{3+}$, one exception is Phe82Ile. The heme crevice of this variant is structurally unstable (Pearce et al., 1989) and may allow the hydrophobic ligands of $Co(phen)_3^{3+}$ to penetrate the protein surface (Louie, 1990).

The use of site-directed mutagenesis as a means of evaluating mechanistic contributions to the reactivity of electron transfer proteins ultimately requires the combined use of structural, electrochemical, and kinetic information as well as a theoretical framework to derive a detailed interpretation of the functional consequences of the mutations involved. The present report in combination with our previous studies (Berghuis et al., 1994a,b; Rafferty et al., 1990) provides such an analysis for two families of cytochrome *c* variants in which regions of the protein believed

to be critical to the electron transfer reactivity of cytochrome *c* have been modified. Our findings establish that this approach can produce detailed mechanistic explanations for the electron transfer reactivity of such variants and that site-directed mutagenesis can be used to modulate mechanistic factors that contribute to this reactivity in a specific and understandable fashion.

SUPPORTING INFORMATION AVAILABLE

Observed rate constants for the reaction of wild-type and variant forms of yeast iso-1-cytochrome *c* with $Fe(EDTA)^{2-}$ and $Co(phen)_3^{3+}$ (14 pages). Ordering information is given on any current masthead page.

REFERENCES

Baker, B. R., Basolo, F., & Neumann, H. M. (1959) *J. Phys. Chem. 63*, 371−378.

Barker, P. D., & Mauk, A. G. (1992) *J. Am. Chem. Soc. 114*, 3619−3624.

Berghuis, A. M., & Brayer, G. D. (1992) *J. Mol. Biol. 223*, 959−976.

Berghuis, A. M., Guillemette, J. G., Smith, M., & Brayer, G. D. (1994a) *J. Mol. Biol. 235*, 1326−1341.

Berghuis, A. M., Guillemette, J. G., McLendon, G., Sherman, F., Smith, M., & Brayer, G. D. (1994b) *J. Mol. Biol. 236*, 786−799.

Cutler, R. L., Pielak, G. J., Mauk, A. G., & Smith, M. (1987) *Protein Eng. 1*, 95−99.

Dutton, P. L. (1978) *Methods Enzymol. 54*, 411−435.

Hendrickson, W. A., & Konnert, J. (1981) in *Biomolecular Structure, Function, Conformation and Evolution* (Sunivasan, R., Ed.) Vol. 1, p 43, Pergamon Press, Oxford.

Hickey, D. R., Berghuis, A. M., Lafond, G., Jaeger, J. A., Cardillo, T. S., McLendon, D., Das, G., Sherman, F., Brayer, G. D., & McLendon, G. (1991) *J. Biol. Chem. 266*, 11686−11694.

Inglis, S. C., Guillemette, J. G., Johnson, J. A., & Smith, M. (1991) *Protein Eng. 4*, 569−574.

Kassner, R. J. (1972) *Proc. Natl. Acad. Sci. U.S.A. 69*, 2263−2267.

Kassner, R. J. (1973) *J. Am. Chem. Soc. 95*, 2674−2677.

Leung, C. J., Nall, B. T., & Brayer, G. D. (1989) *J. Mol. Biol. 206*, 783−785.

Louie, G. V. (1990) Ph.D. Dissertation, University of British Columbia, Vancouver, BC.

Louie, G. V., & Brayer, G. D. (1989) *J. Mol. Biol. 209*, 313−322.

Louie, G. V., & Brayer, G. D. (1990) *J. Mol. Biol. 214*, 527−555.

Louie, G. V., Pielak, G. J., Smith, M., & Brayer, G. D. (1988) *Biochemistry* 27, 7870−7876.

Luzzati, V. (1952) *Acta Crystallogr. 5*, 802−810.

Marcus, R. A., & Sutin, N. (1975) *Inorg. Chem. 14*, 213−216.

Mauk, A. G. (1990) *Struct. Bonding (Berlin) 75*, 131−147.

Michel, B., Mauk, A. G., & Bosshard, H. R. (1989) *FEBS Lett. 243*, 149−152.

Nocek, J. M., Stemp, E. D. A., Finnega, M. G., Koshy, T. I., Johnson, M. K., Margoliash, E., Mauk, A. G., Smith, M., & Hoffman, B. M. (1991) *J. Am. Chem. Soc. 113*, 6822−6831.

Pearce, L. L., Gärtner, A. L., Smith, M., & Mauk, A. G. (1989) *Biochemistry 28*, 3152−3156.

Pielak, G. J., Mauk, A. G., & Smith, M. (1985) *Nature 313*, 152−154.

Przystas, T. J., & Sutin, N. (1973) *J. Am. Chem. Soc. 95*, 5545−5555.

Rafferty, S. P. (1992) Ph.D. Dissertation, University of British Columbia, Vancouver, BC.

Rafferty, S. P., Pearce, L. L., Barker, P. D., Guillemette, J. G., Kay, C. M., Smith, M., & Mauk, A. G. (1990) *Biochemistry 29*, 9365−9369.

Reid, L. S. (1984) Ph.D. Dissertation, University of British Columbia, Vancouver, BC.

Reid, L. S., & Mauk, A. G. (1982) *J. Am. Chem. Soc. 104*, 841−845.

Scott, R. A., & Mauk, A. G., Eds. (1996) *Cytochrome c: A Multidisciplinary Approach*, University Science Books, Mill Valley.

Smith, M., Leung, D. W., Gillam, S., Astell, R., Montgomery, D. L., & Hall, B. D. (1979) *Cell 16*, 753−761.

Takano, T., & Dickerson, R. E. (1981a) *J. Mol. Biol. 153*, 79−94.

Takano, T., & Dickerson, R. E. (1981b) *J. Mol. Biol. 153*, 95−115.

Taniguchi, V. T., Ellis, W. R., Jr., Cammarata, V., Webb, J., Anson, F. C., & Gray, H. B. (1982) in *Electrochemical and Spectrochemical Studies of Biological Redox Components* (Kadish, K. M., Ed.) pp 51−68 Advances in Chemistry Series 201, American Chemical Socity, Washington, DC.

Vogel, A. (1978) *Textbook of Practical Organic Chemistry*, 4th ed., Longman Group Ltd., London.

Wherland, S., & Gray, H. B. (1976) *Proc. Natl. Acad. Sci. U.S.A. 73*, 2950−2954.

Wherland, S., & Gray, H. B. (1977) in *Biological Aspects of Inorganic Chemistry* (Addison, A. W., Cullen, W. R., Dolphin, D., & James, B. R., Eds.) pp 289−368, Wiley, New York.

Wherland, S., Holwerda, R. A., Rosenberg, R. C., & Gray, H. B. (1975) *J. Am. Chem. Soc. 97*, 5260−5262.

Wilkins, R. G., & Yelin, R. E. (1968) *Inorg. Chem. 7*, 2667−2669.

Wilson, A. J. C. (1942) *Nature 150*, 151−152.

Zoller, M. J., & Smith, M. (1983) *Methods Enzymol. 100*, 468−500.

BI960430V